Decision-Feedback Receiver for Quasi-Orthogonal Space-Time Coded OFDM Using Correlative Coding Over Fast Fading Channels

Yu Zhang and Huaping Liu, *Member, IEEE*

Abstract— **Orthogonal frequency division multiplexing (OFDM) is robust against frequency selective fading, but it is very vulnerable to time selective fading. In quasi-orthogonal space-time coded OFDM (ST-OFDM) systems, channel variations cause not only inter-carrier interference among different subcarriers in one OFDM block, but also inter-transmit-antenna interference (ITAI). When applied in fast fading channels, common ST-ODFM receivers usually suffer from an irreducible error floor. In this letter, we apply frequency-domain correlative coding combined with a modified decision-feedback detection scheme to effectively suppress the error floor of quasi-orthogonal ST-OFDM over fast fading channels. The effectiveness of the proposed scheme in mitigating the effects of channel time selectivity is demonstrated through comparison with existing schemes such as zero-forcing, two-stage zero-forcing, and sequential decision feedback estimation.**

Index Terms— **Space-time codes, orthogonal frequency division multiplexing (OFDM), time selective fading, inter-carrier interference (ICI), inter-transmit-antenna interference (ITAI).**

I. INTRODUCTION

ORTHOGONAL frequency division multiplexing (OFDM) is effective in avoiding inter-symbol interference (ISI) caused by multipath delay in a frequency selective environment. One of the disadvantages of OFDM is that it is sensitive to time selective fading, which destroys the orthogonality among different subcarriers in one OFDM block and thus causes inter-carrier interference (ICI) [1], [2]. Multiple antennas can be combined with OFDM to increase diversity gain and to improve spectral efficiency through spatial multiplexing [3]. Performance of multiple-input multiple-output (MIMO) OFDM systems in time selective fading environments was analyzed in [4].

Space-time coding (STC) achieves transmit diversity in multi-antenna systems [5]. Orthogonal space-time block codes (STBCs) were first proposed in [6] for systems with two transmit antennas and later generalized to systems with an arbitrary number of transmit antennas [7]. For more than two transmit antennas, complex orthogonal STBCs with full spatial diversity and full transmission rate do not exist [7], and quasi-orthogonal designs with rate one [8]–[10] could be applied to provide partial diversity. STBCs are typically designed assuming a quasi-static channel, and time selective fading will cause inter-transmit-antenna interference (ITAI) in orthogonal codes. For quasi-orthogonal codes, channel time-variations cause ITAI among all symbols[1], and the pair-wise maximum-likelihood (ML) decoding scheme [8] becomes suboptimal. To mitigate ITAI caused by channel time-variations, many schemes have been studied: a simplified ML decoder for orthogonal STBC with two transmit antennas was proposed to cancel ITAI when the channel varies from one signaling interval to another [11]; a low-complexity receiver was proposed to suppress the bit-error-rate (BER) floor of orthogonal STBC with four transmit antennas using the conventional ML decoding method [12]; a two-step zero-forcing (TS-ZF) scheme was applied to cancel ITAI and to suppress the error floor of quasi-orthogonal STBC [13].

In a MIMO OFDM system over frequency selective fading channels, STC schemes must be extended to include the frequency element, forming space-time coded OFDM (ST-OFDM) [14]. For ST-OFDM systems over fast fading channels, it is necessary to consider the impact of ICI and ITAI simultaneously. The duration of an OFDM symbol in an OFDM system with N_s subcarriers is effectively N_s times of the data symbol period. Thus ITAI caused by channel time-variations in ST-OFDM systems is much more pronounced than in common STC systems. In [15], a sequential decision feedback (DF) sequence estimation (SDFSE) scheme with an adaptive threshold was proposed to mitigate the performance degradation in orthogonal ST-OFDM systems with two transmit antennas over time selective fading channels. However, this scheme does not seem to be very effective in eliminating the error floor. To mitigate ICI caused by channel frequency errors in single-antenna OFDM systems, a simple design using frequency-domain correlative coding was analyzed in [16]. For MIMO OFDM systems, ITAI can be effectively cancelled through a sequential nulling and cancellation process [17], [18] if the number of transmit antennas is less than or equal to the number of receive antennas. Later, a modified decorrelating DF detection scheme was studied in [19] to reduce the complexity and to improve the numerical stability of such schemes.

To effectively mitigate the error floor due to channel time selectivity for ST-OFDM systems, the receiver must deal with both ICI and ITAI. In this letter, we propose a scheme that combines frequency-domain correlative coding and a modified decision-feedback receiver for quasi-orthogonal ST-OFDM systems in time-varying fading environments. We show that the proposed scheme is much more effective in lowering the error floor than existing schemes such as the TS-ZF scheme [13] and the SDFSE scheme [15].

Manuscript received February 1, 2005; revised March 23, 2005; accepted April 20, 2005. The associate editor coordinating the review of this paper and approving it for publication was K. Wong. This paper was presented in part at the IEEE VTC2005-Fall, Sept. 2005.

The authors are with the School of Electrical Engineering and Computer Science, Oregon State University, Corvallis, OR 97331 USA (e-mail: zhangyu@engr.orst.edu; hliu@eecs.orst.edu).

Digital Object Identifier 10.1109/TWC.2006.05054.

[1]With quasi-static fading models, ITAI exists only between pairs of symbols with the 4×4 codes given in [8].

II. System Model

The following notation will be adopted. Column vectors/matrices are denoted by boldface lower/upper case letters; superscripts $(\cdot)^T$, $(\cdot)^*$, and $(\cdot)^H$ denote transpose, complex conjugate, and complex conjugate transpose, respectively; $E[\cdot]$, $var(\cdot)$, and $cov(\cdot)$ stand for expectation, variance, and covariance, respectively; $\boldsymbol{I}_N$ represents the $N \times N$ identity matrix; $\otimes$ denotes Kronecker product; $[\boldsymbol{a}]_p$ denotes the p-th element of vector $\boldsymbol{a}$.

Consider a space-time block coded multi-antenna OFDM system with P transmit antennas, one receive antenna, and N_s subcarriers which employs binary phase shift keying (BPSK) modulation. Input symbols $a_i \in \{1, -1\}$ are assumed independent and identically distributed (i.i.d.). The correlative coding to encode a_i is achieved through the frequency-domain polynomial $F(D) = 1 - D$ [16], which generates a new sequence $b_i = a_i - a_{i-1}$. The encoded sequence $\{b_i,\ i = 0, \cdots, N_sP - 1\}$ is then serial-to-parallel converted into P sequences, each of length N_s, as

$$b_k^{(p)} = b_{k+(p-1)N_s}, \quad p = 1, \cdots, P,\ k = 0, \cdots, N_s - 1. \quad (1)$$

Each of the N_s sequences $\{b_k^{(1)}, \cdots, b_k^{(P)}\},\ k = 0, \cdots, N_s - 1$, is mapped to a matrix $\boldsymbol{\Psi}_k$ of size $P \times P$ by using a quasi-orthogonal space-time block coding scheme (e.g., the 4×4 quasi-orthogonal scheme given in [8]). The transmitted signals are obtained by taking the inverse discrete Fourier transform (DFT) of $\{\boldsymbol{\Psi}_0, \cdots, \boldsymbol{\Psi}_{N_s-1}\}$.

In frequency selective fading channels with L resolvable paths, there exists inter-block interference (IBI). To minimize this IBI, a cyclic prefix of length c_p $(c_p \geq L)$ is added at the beginning of each transmitted OFDM block. In the receiver, the cyclic prefix is discarded, leaving the IBI-free information-bearing signals. Combined with the characteristics of time selective fading, the $N_s \times N_sP$ spatiotemporal channel matrix $\boldsymbol{H}_t$ during the t-th OFDM block period is expressed as shown in Eq. (2) at the top of the next page,[2] where L is less than or equal to N_s and $\boldsymbol{0}$ is a $P \times 1$ zero vector. Each non-zero block of $\boldsymbol{H}_t$ contains the $P \times 1$ channel vector $\boldsymbol{h}_{t,l}(n)$ for path l at time nT_s (T_s is the data symbol period) expressed as

$$\boldsymbol{h}_{t,l}(n) = [h_{t,l}^{(1)}(n), \cdots,\ h_{t,l}^{(P)}(n)]^T,$$
$$l = 0, \cdots, L-1,\ n = 0, \cdots, N_s - 1. \quad (3)$$

If fading is assumed to be quasi-static, which allows the channel coefficients to be constant over an OFDM block and change independently from one block to another, $\boldsymbol{H}_t$ has a block-circulant structure. Without loss of generality, we omit the index of OFDM block period t in the following discussion.

In the special case of quasi-static fading, channel matrix $\boldsymbol{H}$ has the following eigen-decomposition

$$\boldsymbol{H} = \boldsymbol{U}^H \boldsymbol{\Lambda} (\boldsymbol{U} \otimes \boldsymbol{I}_P) \quad (4)$$

where $\boldsymbol{U}$ is the unitary DFT matrix whose (i,j)-th element is given by $u_{ij} = 1/\sqrt{N_s} e^{(-2\pi\sqrt{-1}/N_s)ij}$, $0 \leq i, j \leq N_s - 1$, $\boldsymbol{\Lambda} = diag[\boldsymbol{\lambda}_0^T, \cdots, \boldsymbol{\lambda}_{N_s-1}^T]$ is an $N_s \times N_sP$ block diagonal matrix whose (k,k)-th block is given by

$$\boldsymbol{\lambda}_k = \sum_{l=0}^{L-1} \boldsymbol{h}_l \cdot e^{-\frac{2\pi\sqrt{-1}}{N_s} kl},\ k = 0, \cdots, N_s - 1. \quad (5)$$

Thus the received signals can be obtained as

$$\boldsymbol{x}_k^T = [x_k^{(1)}, \cdots, x_k^{(P)}] = \boldsymbol{\lambda}_k^T \boldsymbol{\Psi}_k + \boldsymbol{w}_k^T,\ k = 0, \cdots, N_s - 1 \quad (6)$$

where $\boldsymbol{w}_k$ is a circularly symmetric zero-mean complex Gaussian noise vector. It is clear from (6) that ICI does not exist in the ST-OFDM system over quasi-static channels.

The P symbols in each column of $\boldsymbol{\Psi}_k$ are transmitted from the P transmit antennas simultaneously during every OFDM block period. If the channel does not change over P consecutive OFDM blocks, the pair-wise ML scheme [8] can be used to detect pairs of transmitted symbols, instead of symbol by symbol, and there is no error floor in BER performance.

III. The Impact of Time-Varying Fading and Decision-Feedback Receiver Design

A. ICI and ITAI caused by time-varying fading

In the presence of time selective fading, $\boldsymbol{H}$ is no longer a block-circulant matrix. Assuming a wide sense stationary uncorrelated scattering (WSSUS) channel [4], all elements of $\boldsymbol{h}_l(n)$ are modeled as independent complex Gaussian random variables with zero mean and equal variance. The channel is assumed to have an exponential power delay profile $\theta(\tau_l) = e^{-\tau_l/\tau_{rms}}$ [20], where τ_l is the delay of the l-th path and τ_{rms} represents the root-mean square delay spread. Since the channel is time-variant, the relationship between the channel coefficients for path l of antenna p at times nT_s and $(n+m)T_s$ can be described by the first-order auto-regressive model as [11], [21]

$$h_l^{(p)}(n+m) = \alpha_m h_l^{(p)}(n) + \beta_l^{(p)}(n+m) \quad (7)$$

where

$$\alpha_m = \frac{E\left[h_l^{(p)}(n) \cdot h_l^{(p)*}(n+m)\right]}{e^{-\frac{\tau_l}{\tau_{rms}}}} = J_0(2\pi m f_d T_s) \quad (8)$$

where f_d is the Doppler shift, $J_0(\cdot)$ is the zero-order Bessel function of the first kind, and $\beta_l^{(p)}(n)$ are independent complex Gaussian random variables with zero mean and variance

$$\sigma_\beta^2 = \begin{cases} 1 - \alpha_m^2, & l = 0 \\ e^{-\frac{\tau_l}{\tau_{rms}}}(1 - \alpha_m^2), & l \neq 0. \end{cases} \quad (9)$$

Consequently, $\boldsymbol{G} = \boldsymbol{U}\boldsymbol{H}(\boldsymbol{U} \otimes \boldsymbol{I}_P)^H$ is no longer a block diagonal matrix as $\boldsymbol{\Lambda}$ given in (4). This shows that time selective fading causes ICI, which is represented by the off-diagonal blocks of $\boldsymbol{G}$. For this more general case, the received signals are given by

$$\boldsymbol{x}_k^T = \boldsymbol{g}_{kk}^T \boldsymbol{\Psi}_k + \sum_{k'=0, k' \neq k}^{N_s-1} \boldsymbol{g}_{kk'}^T \boldsymbol{\Psi}_{k'} + \boldsymbol{w}_k^T, \quad k = 0, \cdots, N_s - 1 \quad (10)$$

where $\boldsymbol{g}_{kk'} = [g_{kk'}^{(1)}, \cdots, g_{kk'}^{(P)}]^T,\ k, k' = 0, \cdots, N_s - 1$, is the (k,k')-th block of $\boldsymbol{G}$. Apparently, the second term on the

[2] The index in the parenthesis following $\boldsymbol{h}_{t,l}$ is the time index.

$$\boldsymbol{H}_t = \begin{bmatrix} \boldsymbol{h}_{t,0}^T(0) & \cdots & \boldsymbol{0}^T & \boldsymbol{h}_{t,L-1}^T(0) & \cdots & \boldsymbol{h}_{t,1}^T(0) \\ \vdots & & & \vdots & & \vdots \\ \boldsymbol{h}_{t,L-1}^T(L-1) & \cdots & \boldsymbol{h}_{t,1}^T(L-1) & \boldsymbol{h}_{t,0}^T(L-1) & \cdots & \boldsymbol{0}^T \\ \vdots & & & \vdots & & \vdots \\ \boldsymbol{0}^T & \cdots & \boldsymbol{h}_{t,L-1}^T(N_s-1) & \cdots & \boldsymbol{h}_{t,1}^T(N_s-1) & \boldsymbol{h}_{t,0}^T(N_s-1) \end{bmatrix} \tag{2}$$

right-hand side of (10) represents ICI. To make the following analysis clearer and easier to understand, we focus on the 4×4 (i.e., $P=4$) quasi-orthogonal STBC given in [8], which is replicated here as

$$\boldsymbol{\Psi}_k = \begin{bmatrix} b_k^{(1)} & -b_k^{(2)*} & -b_k^{(3)*} & b_k^{(4)} \\ b_k^{(2)} & b_k^{(1)*} & -b_k^{(4)*} & -b_k^{(3)} \\ b_k^{(3)} & -b_k^{(4)*} & b_k^{(1)*} & -b_k^{(2)} \\ b_k^{(4)} & b_k^{(3)*} & b_k^{(2)*} & b_k^{(1)} \end{bmatrix}. \tag{11}$$

To decode $\boldsymbol{\Psi}_k$, (10) is processed as

$$\boldsymbol{y}_k = \boldsymbol{M}_{kk}\boldsymbol{\psi}_k + \sum_{k'=0,k'\neq k}^{N_s-1} \boldsymbol{M}_{kk'}\boldsymbol{\psi}_{k'} + \boldsymbol{z}_k \tag{12}$$

where $\boldsymbol{\psi}_k = [b_k^{(1)}, b_k^{(2)}, b_k^{(3)}, b_k^{(4)}]^T$, $\boldsymbol{y}_k = [x_k^{(1)}, x_k^{(2)*}, x_k^{(3)*}, x_k^{(4)}]^T$, $\boldsymbol{z}_k$ is the noise term with the same mean and variance as $\boldsymbol{w}_k$, and the equivalent channel matrix is expressed as

$$\boldsymbol{M}_{kk'} = \begin{bmatrix} \boldsymbol{M}_{kk'}^{(1,2)}(0) & \boldsymbol{M}_{kk'}^{(3,4)}(0) \\ \boldsymbol{M}_{kk'}^{(3,4)*}(2\ell) & -\boldsymbol{M}_{kk'}^{(1,2)*}(2\ell) \end{bmatrix}, \quad k, k' = 0, \cdots N_s - 1 \tag{13}$$

with

$$\boldsymbol{M}_{kk'}^{(i,j)}(n) = \begin{bmatrix} g_{kk'}^{(i)}(n) & g_{kk'}^{(j)}(n) \\ g_{kk'}^{(j)*}(n+\ell) & -g_{kk'}^{(i)*}(n+\ell) \end{bmatrix} \tag{14}$$

where $\ell = N_s + c_p$. By letting $g_{kk'}^{(p)}(0) = g_{kk'}^{(p)},\ p = 1, \cdots, 4$, and using the same first-order auto-regressive model as applied in (7), we have

$$g_{kk'}^{(p)}(q\ell) = J_0(2\pi f_d \ell T_s) g_{kk'}^{(p)}((q-1)\ell) + \varepsilon_{kk'}^{(p)}(q\ell) \tag{15}$$

where the index in the parenthesis following $g_{kk'}^{(p)}$ is the time index and $\{\varepsilon_{kk'}^{(p)}(q\ell)\}$ are independent complex Gaussian random variables with zero mean and variance

$$\sigma_\varepsilon^2 = (1 - J_0^2(2\pi f_d \ell T_s)) \cdot var(g_{kk'}^{(p)}). \tag{16}$$

Let $\boldsymbol{\Upsilon}$ be an $N_s \times N_s$ matrix given by

$$\boldsymbol{\Upsilon} = \begin{bmatrix} var(g_{00}^{(p)}) & \cdots & var(g_{0,N_s-1}^{(p)}) \\ \vdots & \ddots & \vdots \\ var(g_{N_s-1,0}^{(p)}) & \cdots & var(g_{N_s-1,N_s-1}^{(p)}) \end{bmatrix}. \tag{17}$$

As shown in the appendix, for a particular antenna index p, $\boldsymbol{\Upsilon}$ has a circulant structure expressed as

$$\boldsymbol{\Upsilon} = \begin{bmatrix} \gamma_0 & \gamma_1 & \cdots & \gamma_{N_s-1} \\ \gamma_{N_s-1} & \gamma_0 & \cdots & \gamma_{N_s-2} \\ \vdots & \vdots & & \vdots \\ \gamma_1 & \gamma_2 & \cdots & \gamma_0 \end{bmatrix}. \tag{18}$$

Since elements of $\boldsymbol{g}_{kk'},\ k, k' = 0, \cdots, N_s - 1$, are i.i.d. Gaussian random variables [4], (18) applies to all antennas. It is also shown in the appendix that γ_k defined in (18) has a closed-form expression as shown in Eq. (19) at the top of the next page. With (19), $g_{kk'}^{(p)}(q\ell)$ in (15) can be obtained by substituting γ_k into (16). As a result of channel time-variations, $\gamma_k \neq 0$ for $k \neq 0$, which causes ICI. Noteworthily, as mentioned in [16], the frequency-domain correlative coding method incorporated in this letter can effectively enhance system carrier-to-interference ratio without reducing its bandwidth efficiency.

In addition to ICI, channel time-variations in $\boldsymbol{M}_{kk}$ introduce, as mentioned in Section I, additional ITAI among elements of $\boldsymbol{\psi}_k$, which is illustrated as below. If the channel is time-invariant, time indexes of elements in $\boldsymbol{M}_{kk}$ can be omitted and

$$\boldsymbol{M}_{kk}^H \boldsymbol{M}_{kk} = \begin{bmatrix} c & 0 & 0 & d \\ 0 & c & -d & 0 \\ 0 & -d & c & 0 \\ d & 0 & 0 & c \end{bmatrix} \tag{20}$$

where $c = \sum_{p=1}^4 |g_{kk}^{(p)}|^2$ and $d = g_{kk}^{(1)} g_{kk}^{(4)*} + g_{kk}^{(1)*} g_{kk}^{(4)} - g_{kk}^{(2)} g_{kk}^{(3)*} - g_{kk}^{(2)*} g_{kk}^{(3)}$. Apparently, there is no interference between pairs $(b_k^{(1)}, b_k^{(4)})$ and $(b_k^{(2)}, b_k^{(3)})$ [8]. When the channel exhibits time-varying fading, however, (20) does not hold and $\boldsymbol{M}_{kk}^H \boldsymbol{M}_{kk}$ should be expressed as

$$\boldsymbol{M}_{kk}^H \boldsymbol{M}_{kk} = \begin{bmatrix} \varrho_{11} & \varrho_{12} & \varrho_{13} & \varrho_{14} \\ \varrho_{21} & \varrho_{22} & \varrho_{23} & \varrho_{24} \\ \varrho_{31} & \varrho_{32} & \varrho_{33} & \varrho_{34} \\ \varrho_{41} & \varrho_{42} & \varrho_{43} & \varrho_{44} \end{bmatrix} \tag{21}$$

where the non-zero items ϱ_{12} and ϱ_{13} represent the inter-antenna-pair interference to pair $(1,4)$ from pair $(2,3)$. Elements of the first row of matrix $\boldsymbol{M}_{kk}^H \boldsymbol{M}_{kk}$ are expressed as

$$\varrho_{11} = |g_{kk}^{(1)}(0)|^2 + |g_{kk}^{(2)}(\ell)|^2 + |g_{kk}^{(3)}(2\ell)|^2 + |g_{kk}^{(4)}(3\ell)|^2 \tag{22a}$$

$$\varrho_{12} = g_{kk}^{(1)*}(0) g_{kk}^{(2)}(0) - g_{kk}^{(1)*}(\ell) g_{kk}^{(2)}(\ell) + g_{kk}^{(3)}(2\ell) g_{kk}^{(4)*}(2\ell) - g_{kk}^{(3)}(3\ell) g_{kk}^{(4)*}(3\ell) \tag{22b}$$

$$\varrho_{13} = g_{kk}^{(1)*}(0) g_{kk}^{(3)}(0) - g_{kk}^{(1)*}(2\ell) g_{kk}^{(3)}(2\ell) + g_{kk}^{(2)}(\ell) g_{kk}^{(4)*}(\ell) - g_{kk}^{(2)}(3\ell) g_{kk}^{(4)*}(3\ell) \tag{22c}$$

$$\varrho_{14} = g_{kk}^{(1)*}(0) g_{kk}^{(4)}(0) + g_{kk}^{(1)}(3\ell) g_{kk}^{(4)*}(3\ell) - g_{kk}^{(2)}(\ell) g_{kk}^{(3)*}(\ell) - g_{kk}^{(2)*}(2\ell) g_{kk}^{(3)}(2\ell). \tag{22d}$$

B. Decision-feedback receiver design

In a quasi-static fading channel, the received signal can be directly processed by a space-time decoder, whereas in a time-

$$\gamma_k = \frac{1}{N_s^2} \sum_{l=0}^{L-1} \left\{ N_s + 2 \sum_{i=1}^{N_s-1} (N_s - i)\, J_0(2\pi i f_d T_s) \cos\left(\frac{2\pi}{N_s} k i\right) \right\} e^{-\frac{\tau_l}{\tau_{rms}}},\ k = 0, \cdots, N_s - 1 \tag{19}$$

varying fading channel, the detection becomes more complex if ICI and ITAI are to be dealt with simultaneously. The TS-ZF detector [13] aims at lowering the error floor due to ITAI. This scheme will not be very effective for quasi-orthogonal ST-OFDM systems over time-varying channels as ICI could be severe especially when N_s is large.

The SDFSE with an adaptive threshold [15] for two-antenna, orthogonal ST-OFDM systems is expected to perform better than the TS-ZF scheme. But this scheme also suffers from an irreducible error floor. We apply a modified DF scheme for detection of ST-OFDM systems with correlative coding. Without loss of generality, we still focus on the code given in (11) in describing the proposed receiver. The ICI and noise terms in (12) are represented by a single variable $\boldsymbol{d}_k$ as

$$\boldsymbol{d}_k = \sum_{k'=0, k' \neq k}^{N_s-1} \boldsymbol{M}_{kk'} \boldsymbol{\psi}_{k'} + \boldsymbol{z}_k. \tag{23}$$

Then we pre-multiply $\boldsymbol{y}_k$ by $\boldsymbol{\mathcal{L}}^{-1}\boldsymbol{M}_{kk}^H$, which yields

$$\widetilde{\boldsymbol{y}}_k = \boldsymbol{\mathcal{L}}^{-1}\boldsymbol{M}_{kk}^H \boldsymbol{y}_k = \boldsymbol{\mathcal{L}}^H \boldsymbol{\psi}_k + \boldsymbol{e}_k \tag{24}$$

The p-th component of $\widetilde{\boldsymbol{y}}_k$ is given by

$$[\widetilde{\boldsymbol{y}}_k]_p = \boldsymbol{\mathcal{L}}_{pp}^H [\boldsymbol{\psi}_k]_p + \sum_{i=p+1}^{4} \boldsymbol{\mathcal{L}}_{pi}^H [\boldsymbol{\psi}_k]_i + [\boldsymbol{e}_k]_p. \tag{25}$$

The transmitted symbols are detected as

$$\begin{aligned} \widehat{b}_k^{(4)} &= dec\{[\widetilde{\boldsymbol{y}}_k]_4\} \\ \widehat{b}_k^{(p)} &= dec\left\{ [\widetilde{\boldsymbol{y}}_k]_p - \sum_{i=p+1}^{4} \boldsymbol{\mathcal{L}}_{pi}^H \widehat{b}_k^{(i)} \right\}, \quad p = 1, 2, 3 \end{aligned}$$

where $dec(\cdot)$ is the slice function corresponding to $(1 - D)$ correlative coding [16]. Finally, $\{a_i\}$ can be recovered by using a ML sequence detector [23].

It is well known that performance of the DF scheme described above can be significantly improved if signals are ranked according to their relative strength[3] and then followed by a successive cancellation process [17], [18]. The decorrelating DF detection scheme [19] for spatial multiplexing systems requires that the number of receive antennas be greater than or equal to the number of transmit antennas. Since the equivalent channel matrix $\boldsymbol{\mathcal{L}}^H$ in (24) is a 4×4 matrix, this DF scheme can be employed for detection of quasi-orthogonal ST-OFDM systems in time-varying environments. The detection begins with (24) by decoding the strongest signal first and then followed by a cancellation process, which is summarized as follows. Let $\boldsymbol{\mathcal{L}}^{(u)}|_{u=4} = \boldsymbol{\mathcal{L}}$. The following procedures are repeated for $u = 4$ to 1:

1) *Find the column of* $(\boldsymbol{\mathcal{L}}^{(u)})^{-1}$ *which has the smallest column norm, and exchange it with the last column via a unitary transformation* $\boldsymbol{\mathcal{P}}$ *as* $(\boldsymbol{\mathcal{L}}^{(u)})^{-1}\boldsymbol{\mathcal{P}}$.
2) *Find a unitary matrix* $\boldsymbol{\mathcal{O}}$ *which transforms* $\boldsymbol{\mathcal{L}}^{(u)*}\boldsymbol{\mathcal{P}}$ *to an upper triangular matrix* $\boldsymbol{\mathcal{O}}\boldsymbol{\mathcal{L}}^{(u)*}\boldsymbol{\mathcal{P}}$. *Then, compute the lower triangular matrix* $\boldsymbol{\mathcal{O}}(\boldsymbol{\mathcal{L}}^{(u)})^{-1}\boldsymbol{\mathcal{P}}$.
3) *Perform DF detection based on (24) using the reordered matrices.*

Because this modified DF detection scheme guarantees that the detected signal has the highest SNR at every step, it should achieve a better BER performance than conventional DF schemes.

[3]The strongest signal refers to the signal with the highest signal-to-noise ratio (SNR), and the weakest signal refers to the signal with the lowest SNR.

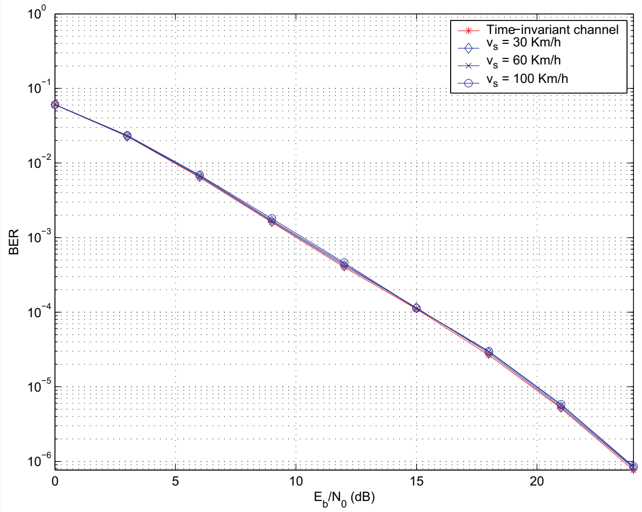

Fig. 1. BER versus E_b/N_0 for quasi-orthogonal ST-OFDM systems with different fading rates ($N_s = 16$, $T_s = 10^{-6}$s).

IV. Simulation Results and Discussion

Simulations are carried out based on the "SUI-5" channel model [24], which is one of six channel models adopted by IEEE 802.16a for evaluating broadband wireless systems in the 2-11GHz band. We consider a system with four transmit antennas and one receive antenna which employs BPSK modulation and the 4×4 quasi-orthogonal STBC given in (11). The time selective Rayleigh fading channel is assumed to have three resolvable multipath components, each of which at 0, 5, and $10\mu s$ is modeled as an independent complex gaussian random variable. The rms delay spread is $3.05\mu s$, and the Doppler shift of the channel is calculated based on a carrier frequency of $f_c = 2$GHz.

Fig. 1 shows the simulated BER performance of the system which employs the modified DF detection scheme. The OFDM symbol is assumed to have $N_s = 16$ subcarriers, and each data symbol period is $T_s = 10^{-6}$ seconds. Performances with different vehicle speeds evaluated, $v_s = 30, 60,$ and 100Km/h, are compared. In the same figure, the curve of the quasi-orthogonal ST-OFDM system over a time-invariant multipath fading channel is used as the baseline performance. When the number of subcarriers is small ($N_s = 16$ in Fig. 1), the system performs almost the same for any of the vehicle speeds, all of which approach the baseline performance.

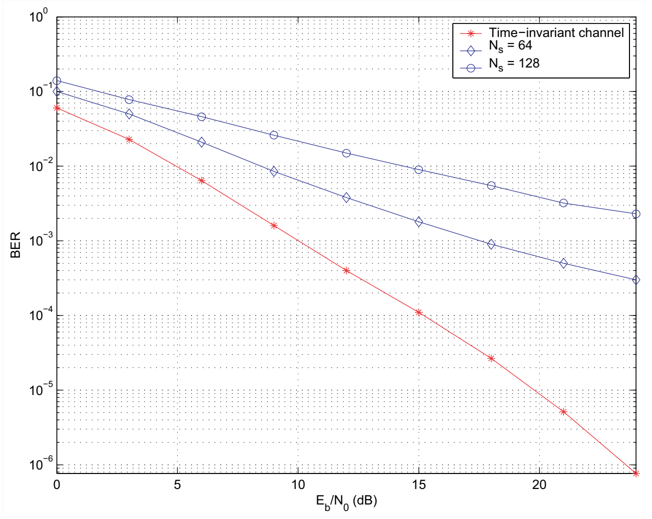

Fig. 2. BER versus E_b/N_0 for quasi-orthogonal ST-OFDM systems with different number of subcarriers ($v_s = 100$Km/h, $T_s = 10^{-6}$s).

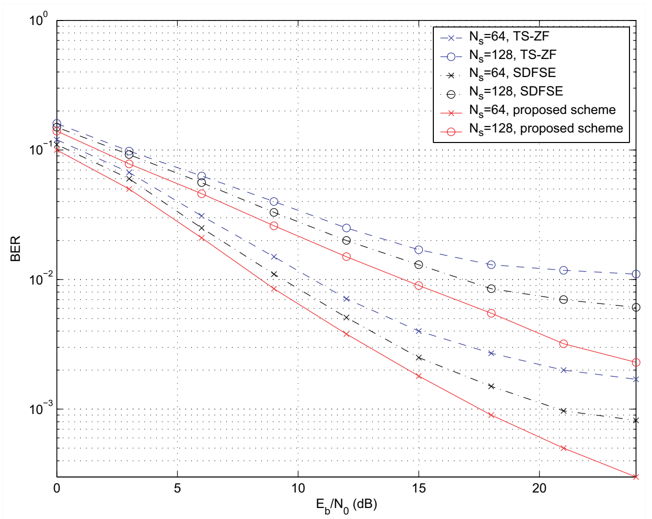

Fig. 3. Error performances of the quasi-orthogonal ST-OFDM system with different detection schemes.

As the number of subcarriers increases, however, system performance deteriorates rapidly. This is clearly shown in Fig. 2, where the vehicle speed is $v_s = 100$Km/h and all other parameters are the same as those applied to generate Fig. 1. From the BER versus E_b/N_0 curves with $N_s = 64$ and 128, the error floor becomes larger as N_s increases. The main reason is that a larger number of subcarriers within one OFDM block not only causes a more severe ICI but also increases the time interval in (16), causing a greater amount of ITAI within one STBC matrix.

In Fig. 3, we compare the performances of three different schemes: the TS-ZF, the SDFSE, and the proposed scheme which uses frequency-domain correlative coding and the modified DF detection scheme. All parameters are the same as those applied for Fig. 2. It is observed that the proposed scheme effectively eliminates the error floor of the quasi-orthogonal ST-OFDM system, whereas the TS-ZF and the SDFSE schemes both suffer from an error floor.

The required number of metric calculations for an quasi-orthogonal STBC codeword (4 consecutive OFDM symbol periods) with the TS-ZF scheme is proportional to QN_s [13], where Q is the constellation size. The number of metric calculations for the same codeword with the SDFSE scheme approximately equals $Q^{2q}N_s$ [15], where $2q$ is the number of subchannels that cause inter-codeword couplings. The computational complexity of the proposed scheme is approximately P^3N_s. With a typical set of system parameters (e.g., $Q = 2$, $P = 4$, and $q = 3$), the TS-ZF scheme has the lowest complexity, and the SDFSE scheme with an adaptive threshold and the proposed scheme have comparable complexities.

V. Conclusion

We have studied a scheme that combines frequency-domain correlative coding with a modified decision-feedback receiver for quasi-orthogonal ST-OFDM systems over time selective fading channels. We have analyzed the impact of channel time selectivity on the performance of such systems. Performances of three detection schemes are compared, and it is found that the proposed scheme can effectively eliminate the error floor of quasi-orthogonal ST-OFDM systems in fast fading environments.

Appendix
Proof That $\boldsymbol{\Upsilon}$ is a Circulant Matrix and Derivation of (19)

Since $\boldsymbol{\Upsilon}$ in (17) is the same for any antenna index p, we can replace vector $\boldsymbol{h}_l(n)$ of the channel matrix $\boldsymbol{H}$ in (2) with a scalar $h_l^{(p)}(n)$ (note that OFDM block index is omitted for notational simplicity) and replace zero vector $\mathbf{0}$ with scalar 0, forming a new $N_s \times N_s$ matrix $\boldsymbol{\mathcal{H}}$. Let us also define

$$\begin{aligned} \boldsymbol{\mathcal{G}} &= \{g_{ij}^{(p)},\ i,j = 0,\cdots,N_s-1\} = \boldsymbol{U}\boldsymbol{\mathcal{H}}\boldsymbol{U}^H \\ \boldsymbol{\Upsilon} &= \{\gamma_{ij}^{(p)}\} = \{var(g_{ij}^{(p)})\} \end{aligned} \tag{26}$$

where $\boldsymbol{U}$ is the DFT matrix defined in (4). We note that $\boldsymbol{U} = \{u_{ij}\} = [\boldsymbol{u}_0,\cdots,\boldsymbol{u}_{N_s-1}]$. Since $\boldsymbol{\Upsilon}$ is independent of p, we omit antenna index p in the following discussion. If we denote $\boldsymbol{\mathcal{H}}$ as the sum of L matrices as $\boldsymbol{\mathcal{H}} = \sum_{l=0}^{L-1}\boldsymbol{\mathcal{H}}_{(l)}$, where $\boldsymbol{\mathcal{H}}_{(l)}$ is a matrix formed by cyclic left-shifting the diagonal matrix $diag\{h_l(0),\cdots,h_l(N_s-1)\}$ by l columns, we have

$$\boldsymbol{\mathcal{G}} = \sum_{l=0}^{L-1}\boldsymbol{\mathcal{G}}_l = \sum_{l=0}^{L-1}\boldsymbol{U}\boldsymbol{\mathcal{H}}_{(l)}\boldsymbol{U}^H \tag{27}$$

where $\boldsymbol{\mathcal{G}}_l = \{g_{l,ij}\}$. With the conditions expressed in Eq. 28 at the top of the next page

$$\begin{aligned} E\left[h_l(n)\right] &= 0,\ l = 0,\cdots,L-1, \\ &\quad\ n = 0,\cdots,N_s-1 \\ E\left[h_l(r)\cdot h_{l'}^*(s)\right] &= J_0(2\pi|r-s|f_dT_s)\delta_{l-l'}e^{-\frac{\tau_l}{\tau_{rms}}}, \\ &\quad\ r,s = 0,\cdots,N_s-1 \end{aligned} \tag{28}$$

it is recognized that $\boldsymbol{\Upsilon} = \sum_{l=0}^{L-1}\boldsymbol{\Upsilon}_l$, where $\boldsymbol{\Upsilon}_l = \{\gamma_{l,ij}\} = \{var(g_{l,ij})\}$. Since the sum of circulant matrices of the same dimension is also a circulant matrix, we only need to prove that each $\boldsymbol{\Upsilon}_l$ is a circulant matrix.

For any integer n, let $[n]$ denotes n modulo N_s. Note that

$$g_{l,ij} = \boldsymbol{u}_i^T\boldsymbol{\mathcal{H}}_{(l)}\boldsymbol{u}_j^* = \boldsymbol{\eta}_{ij}^T\boldsymbol{h}_l \tag{29}$$

$$\begin{aligned}\gamma_{ij} &= \sum_{l=0}^{L-1}\gamma_{l,ij} = \frac{1}{N_s^2}\sum_{l=0}^{L-1}\sum_{r=0}^{N_s-1}\sum_{s=0}^{N_s-1} J_0(2\pi|r-s|f_dT_s)e^{-(2\pi\sqrt{-1}/N_s)t_{ijrs}}e^{-\frac{\tau_l}{\tau_{rms}}}\\ &= \frac{1}{N_s^2}\sum_{l=0}^{L-1}\left\{N_s + 2\sum_{m=1}^{N_s-1}(N_s-m)J_0(2\pi m f_d T_s)\cos\left(\frac{2\pi}{N_s}[j-i]m\right)\right\}e^{-\frac{\tau_l}{\tau_{rms}}} \quad (31)\end{aligned}$$

where $\boldsymbol{\eta}_{ij} = [\eta_{ij0}, \cdots, \eta_{ij,(N_s-1)}]^T$, $\eta_{ijn} = u_{in}u^*_{j,[n-l]}$, and $\boldsymbol{h}_l = [h_l(0), \cdots, h_l(N_s-1)]^T$. Thus

$$\begin{aligned}\gamma_{l,ij} &= var(\boldsymbol{\eta}_{ij}^T\boldsymbol{h}_l) = \sum_{r=0}^{N_s-1}\sum_{s=0}^{N_s-1}\eta_{ijr}\chi(r,s)\eta^*_{ijs}\\ &= \frac{1}{N_s^2}\sum_{r=0}^{N_s-1}\sum_{s=0}^{N_s-1}\chi(r,s)e^{-(2\pi\sqrt{-1}/N_s)t_{ijrs}} \quad (30)\end{aligned}$$

where $\chi(r,s) = cov(h_l(r)\cdot h_l^*(s))$ and $t_{ijrs} = ir - j[r-l] - is + j[s-l]$. It suffices to show, for any fixed r and s, that $[t_{ijrs}] = [ir - j[r-l] - is + j[s-l]] = [j-i][s-r]$.

Also note that an $N_s \times N_s$ matrix $\boldsymbol{B} = \{b_{ij}\}$, $0 \le i,j \le N_s - 1$, is circulant if and only if $b_{ij} = \kappa_{[j-i]}$, i.e., if and only if b_{ij} depends only on $[j-i]$ and $e^{-(2\pi\sqrt{-1}/N_s)k} = e^{-(2\pi\sqrt{-1}/N_s)[k]}$ because $e^{2\pi\sqrt{-1}} = 1$. Thus from (30), we can conclude that $\boldsymbol{\Upsilon}_l$ is a circulant matrix if $h_l(n)$, $n = 0, \cdots, N_s-1$, are finite.

Moreover, from (30) we have (31) at the top of this page.

REFERENCES

[1] M. Russell and G. J. Stüber, "Interchannel interference analysis of OFDM in a mobile environment," in *Proc. IEEE Vehicular Technology Conf. 1995*, pp. 820–824.

[2] J. Li and M. Kavehrad, "Effects of time selective multipath fading on OFDM systems for broadband mobile applications," *IEEE Commun. Lett.*, vol. 3, pp. 332–334, Dec. 1999.

[3] G. J. Stüber, J. R. Barry, S. W. Mclaughlin, Y. Li, M. A. Ingram, and T. G. Pratt, "Broadband MIMO-OFDM wireless communications," *Proc. IEEE*, vol. 92, pp. 271–294, Feb. 2004.

[4] A. Stamoulis, S. N. Diggavi, and N. AL-Dhahir, "Intercarrier interference in MIMO OFDM," *IEEE Trans. Signal Processing*, vol. 50, pp. 2451–2464, Oct. 2002.

[5] V. Tarokh, N. Seshadri, and A. R. Calderbank, "Space-time codes for high data rate wireless communication: Performance criterion and code construction," *IEEE Trans. Inform. Theory*, vol. 44, pp. 744–765, Mar. 1998.

[6] S. M. Alamouti, "A simple transmit diversity technique for wireless communications," *IEEE J. Select. Areas Commun.*, vol. 16, pp. 1451–1458, Oct. 1998.

[7] V. Tarokh, H. Jafarkhani, and A. R. Calderbank, "Space-time block codes from orthogonal designs," *IEEE Trans. Inform. Theory*, vol. 45, pp. 1456–1467, July 1999.

[8] H. Jafarkhani, "A quasi-orthogonal space-time block code," *IEEE Trans. Commun.*, vol. 49, pp. 1–4, Jan. 2001.

[9] O. Tirkkonen, A. Boariu, and A. Hottinen, "Minimal non-orthogonality rate 1 space-time block code for 3+ tx antennas," in *Proc. IEEE ISSSTA 2000*, pp. 429–432.

[10] J. Hou, M. H. Lee, and J. Y. Park, "Matrices analysis of quasi-orthogonal space-time block codes," *IEEE Commun. Lett.*, vol. 7, pp. 385–387, Aug. 2003.

[11] T. A. Tran and A. .B. Sesay, "A generalized simplified ML decoder of orthogonal space-time block code for wireless communications over time-selective fading channels," in *Proc. IEEE Vehicular Technology Conf. 2002*, pp. 1911–1915.

[12] F. -C. Zheng and A. G. Burr, "Receiver design for orthogonal space-time block coding for four transmit antennas over time-selective fading channels," in *Proc. GLOBECOM 2003*, pp. 128–132.

[13] F. -C. Zheng and A. G. Burr, "Signal detection for non-orthogonal space-time block coding over time-selective fading channels," *IEEE Commn. Lett.*, vol. 8, pp. 491–493, Aug. 2004.

[14] M. Uysal, N. AL-Dhahir, and C. N. Georghiades, "A space-time block-coded OFDM scheme for unknown frequency-selective fading channels," *IEEE Commun. Lett.*, vol. 5, pp. 393–395, Oct. 2001.

[15] J. Kim, R. W. Heath, Jr., and E. J. Powers "Receiver designs for Alamouti coded OFDM systems in fast fading channels," to appear in *IEEE Trans. Wireless Commun.*

[16] Y. Zhao and S. G. Häggman, "Intercarrier interference compression in OFDM communication systems by using correlative coding," *IEEE Commun. Lett.*, vol. 2, pp. 214–216, Aug. 1998.

[17] G. D. Golden, C. J. Foschini, R. A. Valenzuela, and P. W. Wolniansky, "Detection algorithm and initial laboratory results using V-BLAST space-time communication architecture," *Electron. Lett.*, vol. 35, pp. 14–16, Jan. 1999.

[18] B. Hassibi, "A fast square-root implementation for BLAST," in *Proc. 34th Asilomar Conference on Signal, Systems, and Computers 2000*, pp. 1255–1259.

[19] W. Zha and S. D. Blostein, "Modified decorrelating decision-feedback detection of BLAST space-time system," in *Proc. ICC 2002*, vol. 1, pp. 335–339.

[20] O. Edfors, M. Sandell, J. -J. v. d. Beek, S. K. Wilson, and P. O. Börjesson, "OFDM channel estimation by singular value decomposition," *IEEE Trans. Commun.*, vol. 46, pp. 931–939, July 1998.

[21] R. H. Clarke, "A statistical theory of mobile radio reception," *Bell Syst. Tech. J.*, vol. 47, pp. 957–1000, July 1968.

[22] H. Moose, "A technique for orthogonal frequency division multiplexing frequency offset correction," *IEEE Trans. Commun.*, vol. 42, pp. 2908–2914, Oct. 1994.

[23] G. D. Forney, Jr., "Maximum-likelihood sequence estimation of digital sequences in the presence of intersymbol interference," *IEEE Trans. Inform. Theory*, vol. 18, pp. 363–378, May 1972.

[24] D. Falconer, S. L. Ariyavisitakul, A. Benyamin-Seeyar, and B. Eidson, "Frequency domain equalization for single-carrier broadband wireless systems," *IEEE Commun. Mag.*, vol. 40, pp. 58–66, Apr. 2002.